J. Fluid Mech. (1977), *vol.* 79, *part* 3, *pp.* 435–447
Printed in Great Britain

The flow of a stratified fluid in a rotating annulus

By P. F. LINDEN

Department of Applied Mathematics and Theoretical Physics,
University of Cambridge

(Received 19 January 1976 and in revised form 26 July 1976)

The motion of a continuously stratified fluid in a rotating annulus is investigated experimentally. The flow is driven by the differential rotation of a lid on the annulus in contact with the fluid. For small enough Rossby numbers the basic flow is found to be axisymmetric, but in contrast to the unstratified case the zonal flow is not independent of the depth, and there is significant vertical shear in the interior. As the Rossby number of the flow is increased the axisymmetric flow becomes unstable to non-axisymmetric baroclinic disturbances. Some features of these disturbances as well as the time response to the motion of the lid are examined.

1. Introduction

An understanding of the combined effects of rotation and density stratification is fundamental to many geophysical flows. When the fluid is homogeneous and the Coriolis force is large compared with the viscous and inertia forces, the Taylor–Proudman (1917) theorem states that the velocity does not vary in the direction of the rotation vector. However, if the fluid is stratified the Taylor–Proudman theorem and the constraints that it imposes on the flow do not apply. Consequently a rotating stratified fluid can support significant vertical shears even if the rotation axis is vertical.

When a column of fluid is extended (or compressed) in a rotating fluid, changes in vorticity occur. A stable density stratification inhibits vertical motions and so homogeneous flows, which rely on vertical extensions of fluid columns to change the vorticity of the fluid, may be altered quite drastically by the stratification. Horizontal variations in density can also produce many interesting motions in a rotating fluid. These horizontal density gradients may either be produced by external boundary conditions or arise from the internal dynamics in response to some forcing. They provide a source of energy which may be released under appropriate conditions, the so-called baroclinic instabilities, to produce a wide range of interesting and important phenomena.

This paper describes some experiments on the motion of a stratified fluid in a rotating annulus. The flow is driven mechanically by the differential rotation of a lid on the annulus. The stratification is produced by changes in the concentration of a dissolved solute, and all the boundaries are impermeable to this solute, i.e., to use the thermal analogy, all the boundaries are 'insulating'. The flow exhibits each of the features mentioned above and we examine them in turn. In

§ 2 the experimental apparatus and techniques are described. The steady-state flow fields are discussed in § 3 and the transient response to the boundary forcing is described in § 4. Non-axisymmetric baroclinic motions observed in some of the experiments are examined in § 5 and some conclusions are presented in § 6.

2. The experiments

The experiments were carried out in a cylindrical Perspex tank mounted on a rotating table. A cylindrical aluminium hub was fitted in the centre of the tank, thereby producing an annular working section. The inner and outer radii of the annulus were 15·2 and 45·7 cm, respectively, and the working depth of the tank was 14·2 cm. The axes of symmetry of the hub and the cylinder were coincident with the vertical rotation axis of the table. The tank was filled with an aqueous sugar solution such that the density decreased linearly from the bottom to the top. This density stratification was achieved by the use of a 'double-bucket' system (Oster 1965) modified to allow the tank to be filled whilst rotating. The two storage tanks were fixed in the laboratory frame, and the fluid was added to the tank by pouring it into a funnel at the top of a filling tube passing down through the central hub along the rotation axis. The fluid then entered the tank via a small gap at the bottom of the inner wall of the annulus. Mixing with fluid already in the annulus was kept to a minimum by some sponge rubber in the gap between the hub and the bottom of the tank.

The flow in the annulus was driven by a lid on the tank, in contact with the fluid, which was rotated relative to the tank. This meant that the lid could not be fixed to the outer wall of the tank, and it was necessary to remove the air trapped under the lid during the filling process. As the tank was filled whilst it was rotating, the centrifugal force kept the air trapped under the lid near the centre of the tank, and so small holes were drilled into the filling tube between the hub and the lid. Small tubes connected these holes to a thin pipe placed concentrically in the filling tube. A rotating seal was attached to the top of this central pipe and the trapped air was removed by sucking this pipe during the last stages of the filling process. By this method all the air was removed from the annulus, although occasionally some air would remain trapped over the hub. As the gap between the hub and the lid was less than 0·1 cm it is thought that this air did not affect the flow in the annulus. A sketch of the tank and the filling arrangement is shown in figure 1.

The flow was visualized by using Thymol blue, an indicator which changes from orange to blue when its pH is increased. The required increase in pH can be achieved by placing cathodic electrodes in the solution (Baker 1966). In the present experiments an electrode consisted of a horizontal wire stretched across a radius vector. Attached to this wire were 1 cm long vertical pieces of wire at 2 cm horizontal spacing. When a potential difference of approximately 12 V was applied between the wire and a positive electrode on the side of the tank, blue dye was swept from the wire by the flow. When viewed from above this dye marked the horizontal streamlines of the flow. Six of these electrodes were placed at different depths across the annulus (see figure 10, plate 1).

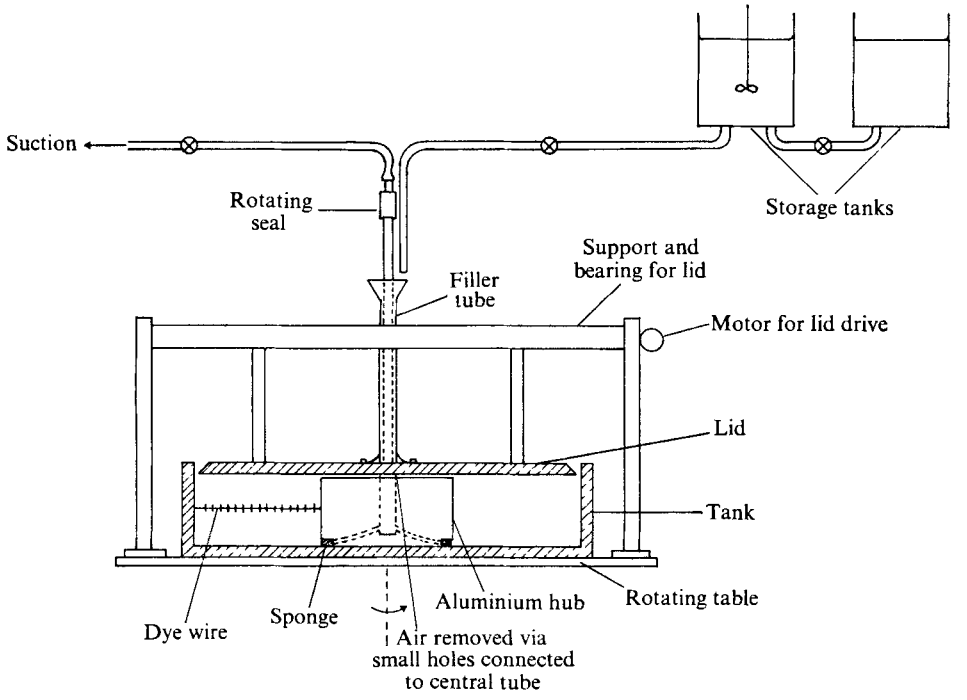

FIGURE 1. A sketch of the experimental apparatus.

These dye lines were photographed from above by a camera mounted on the rotating table. The current to the electrodes was switched on and the dye lines were photographed at known intervals of time measured with a stop-watch to within 0·1 s. Measurements of the position of the start of the dye at different times were then translated into azimuthal and radial velocities, as functions of radius and depth, the latter depending on which electrode was supplied with current. By running through each of the six electrodes in turn it was possible to get three measurements of the velocity field at each depth. This limit was set by the camera as it was necessary to stop the tank from rotating to change films after 36 exposures, and this destroyed the stratification.

The main errors involved in determining the velocities came from two sources: the identification of the position of the end of the dye line and parallax. The former were minimized by photographing the dye lines relatively close to the electrode. Parallax was allowed for when analysing the photographs. It is estimated that the velocities are accurate to within 15 % and the measurements were reproducible within this limit.

The experimental procedure was as follows. Solutions of the required density were mixed in the storage tanks and the Thymol blue titrated to its end point. These solutions were then left to stand for at least 12 h to come to room temperature. The tank was set rotating at the desired rate and then filling began. Typically, the flow rate was adjusted such that it took about 5 h to fill the tank. It was estimated that this rate was the maximum that could be achieved without mixing. A strong zonal flow was present after filling and the lid was kept stationary

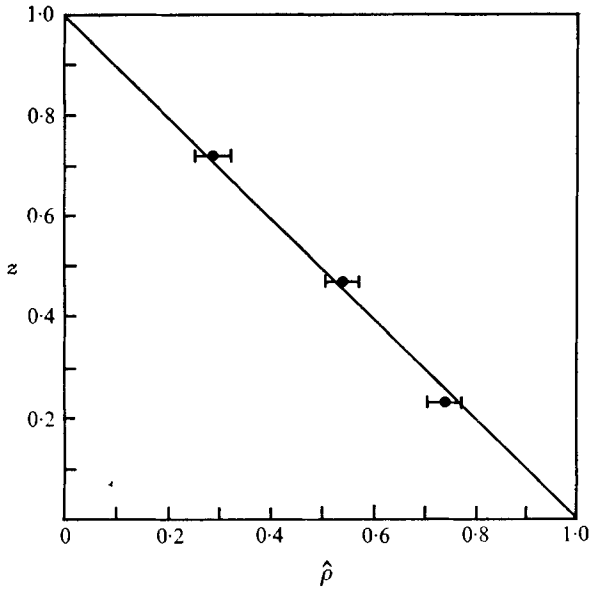

FIGURE 2. A plot of the non-dimensional density $\hat{\rho}$, defined by

$$\hat{\rho}(z) = (\rho(z) - \rho(1))/(\rho(0) - \rho(z)),$$

against the non-dimensional depth z. The points represent the mean of the values measured in all the runs at a particular depth. The solid line represents the intended density distribution.

until this had decayed to a negligible strength,† which usually took 2–3 h. At this time samples (2 ml) were withdrawn at three different depths in the tank, via stainless-steel tubes attached to syringes fixed to the rotating table. The lid was then set in motion and the flow monitored at discrete times thereafter. When the experiment had been completed the samples were recovered and analysed.

The density of each sample was determined by measuring its refractive index and converting this measurement to density by calibration. The calibration was reproducible to within 0·5 %. As the densities at the top and bottom of the tank were known from the initial and final densities of the fluid in the storage tanks, each profile is determined by five readings. In all but one case (the result of a spill during filling and excluded from the subsequent discussion) the density gradient was found to be a constant, within experimental accuracy, over the depth of the tank. This can be seen on figure 2, which is a plot of the non-dimensional density $\hat{\rho}(z)$ against the non-dimensional depth z. $\hat{\rho}(z)$ is defined by

$$\hat{\rho}(z) = \frac{\rho(z) - \rho(1)}{\rho(0) - \rho(z)}, \quad 0 \leqslant z \leqslant 1,$$

and so all density profiles pass through the points (0, 1) and (1, 0) in the $\hat{\rho}, z$ plane. Figure 2 represents a summary of all the profiles from the different experiments and the data show that the intended density profile (the solid line) was achieved in practice.

† Some flow is always present in a rotating stratified fluid; see § 4.

Reference is made to a cylindrical co-ordinate system (r, θ, z) with $r = 0$ coinciding with the axis of rotation. The velocity field in these co-ordinates is given by $\mathbf{u} = (u, v, w)$. Length scales are non-dimensionalized with respect to the depth H, the annular region occupying $1{\cdot}07 < r < 3{\cdot}22$, $0 \leqslant \theta \leqslant 2\pi$, $0 < z < 1$. Let Ω represent the rotation rate of the tank, ω the relative angular velocity of the lid, ρ the density of the fluid, ν its kinematic viscosity and κ the coefficient of molecular diffusion. A convenient measure of the stratification is the buoyancy frequency $N = (-g\rho_0^{-1} d\rho/dz)^{\frac{1}{2}}$, where g is the gravitational acceleration and ρ_0 a mean density. In these experiments N was independent of z.

From these physical parameters we can define the following non-dimensional parameters of the flow: $\epsilon = \omega/2\Omega$, the Rossby number; $E = \nu/\Omega H^2$, the Ekman number; $\sigma = \nu/\kappa$, the Prandtl number, and $S = N^2/\Omega^2$, the stratification parameter. In the experiments these parameters took the following values:

$$0{\cdot}0013 \leqslant \epsilon \leqslant 0{\cdot}44, \quad 3{\cdot}1 \times 10^{-5} \leqslant E \leqslant 7{\cdot}8 \times 10^{-5}, \quad 0 \leqslant S \leqslant 17{\cdot}9, \quad \sigma \doteq 2 \times 10^3.$$

3. The mean flow

In an unstratified rotating fluid ($S = 0$) at low Rossby and Ekman numbers ($\epsilon \ll 1$, $E \ll 1$) the flow in an annulus driven by a differentially rotating lid is known to consist of two regions: an interior region where the flow is independent of depth, and boundary layers, on the side walls and the top and bottom of the annulus, in which the velocity field adjusts to satisfy the no-slip conditions on the boundaries. In the interior, linear theory predicts that $u = O(E)$, $v = \frac{1}{2}\omega r$ and $w = O(E^{\frac{1}{2}})$. Figure 3 shows the zonal velocity measured at the mid-radius of the annulus for the unstratified ($S = 0$) flow with $\epsilon = 0{\cdot}04$ and $E = 5{\cdot}2 \times 10^{-4}$. The experimental results are in excellent agreement with linear theory, which predicts a depth-independent interior flow with zonal velocity, at a given radius, equal to one-half the velocity of the lid. The top and bottom Ekman layers of thickness $O(E^{\frac{1}{2}})$, in which the zonal velocity has a large gradient in order to satisfy the no-slip conditions, are too thin to be revealed by the measurement technique. When $S = 0$, the motion of the lid is transmitted to the interior by a small, $O(E^{\frac{1}{2}})$ vertical velocity which is independent of depth.

When the fluid is stratified ($S > 0$) the stable density gradient in the interior tends to inhibit this vertical motion. Consequently, for large enough values of the stratification parameter S, the Ekman layers do not play a significant role in the dynamics and the interior azimuthal velocity must satisfy the no-slip boundary conditions on the top and bottom boundaries.

In the case of steady flow, the effect of stratification is most easily seen by reference to the buoyancy equation

$$\epsilon \mathbf{u} \cdot \nabla \rho' + w\sigma S = E\nabla^2 \rho', \tag{3.1}$$

where ρ' is the perturbation density. In the interior the vertical advection w necessary to balance the diffusion of density is $O(E/\sigma S)$. This is smaller than the Ekman velocity $w = O(E^{\frac{1}{2}})$ when $\sigma S > E^{\frac{1}{2}}$, in which case it is expected that the flow will be significantly different from the homogeneous case. Unfortunately,

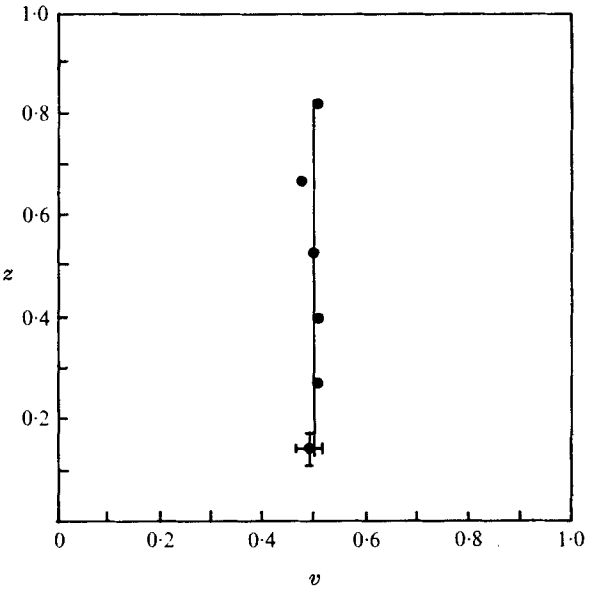

FIGURE 3. The azimuthal velocity v (non-dimensionalized with respect to the velocity of the lid) at (nominal) mid-radius, plotted against the non-dimensional height, for the unstratified case $S = 0$. In this case $\epsilon = 0{\cdot}04$ and $E = 5{\cdot}2 \times 10^{-4}$. The solid line represents the interior velocity as determined from linear theory. The error bars represent the maximum possible uncertainty in the measurements.

owing to the large Prandtl number associated with the sugar stratification ($\sigma \approx 10^3$) it was not possible to examine the flow in the parameter regime $E^{\frac{1}{2}}/\sigma S = O(1)$. This would have meant setting up a stratification with a density difference between the top and bottom of the tank $\Delta\rho/\rho_0 \sim 10^{-7}$, and this was impossible with the present apparatus. Therefore, except for the homogeneous case ($S = 0$) only strongly stratified flows, with $\sigma S \gg E^{\frac{1}{2}}$, were examined.

The most striking effect of the stratification is seen in the profiles of the azimuthal velocity v *vs.* depth. Figures 4, 5 and 6 show examples of these profiles for a range of Rossby numbers and stratification parameters. The velocity at mid-radius is shown, non-dimensionalized by the velocity of the lid at that radius. In each case the zonal velocity has an $O(1)$ vertical shear in the interior, in contrast to the uniform velocity found in homogeneous fluid. On figure 6, three profiles measured for the same values of S and E but with different Rossby numbers ϵ are shown. There appears to be no significant variation in the mean profile with ϵ up to $7{\cdot}5 \times 10^{-3}$. A more detailed picture of the zonal velocity field is obtained from contours of v in the r, z plane. A typical contour plot is shown on figure 7. The penetration of the surface velocity into the interior is clearly visible.

The profiles shown on figures 4, 5 and 6 are for $S = 0{\cdot}36$, $0{\cdot}63$ and $0{\cdot}86$, respectively. Bearing in mind that $v(r, 0) = 0$ and $v(r, 1) = 1$, we see that the interior zonal velocity approaches its boundary values smoothly, except perhaps for the most weakly stratified case $S = 0{\cdot}36$. In the profile shown on figure 4 there is some evidence of a larger vertical shear at the top, which is indicative of an Ekman layer near the lid. The other two profiles and the contour plots

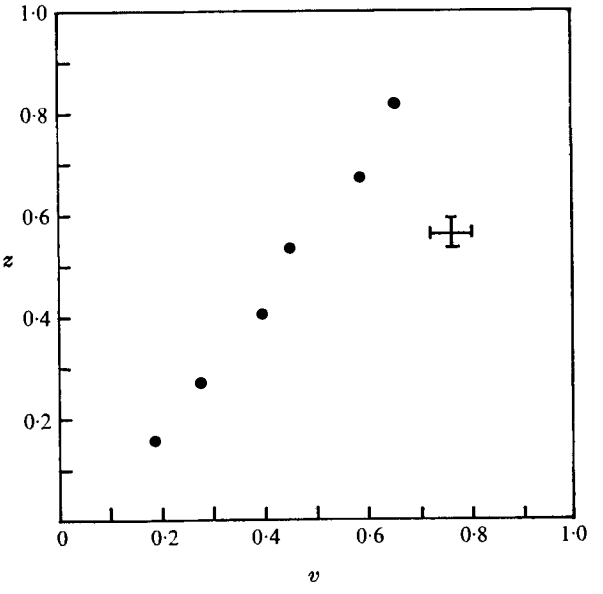

FIGURE 4. The same quantities as are plotted on figure 3. Here the flow is stratified with $S = 0{\cdot}36$, $\epsilon = 1{\cdot}6 \times 10^{-3}$ and $E = 4{\cdot}8 \times 10^{-4}$.

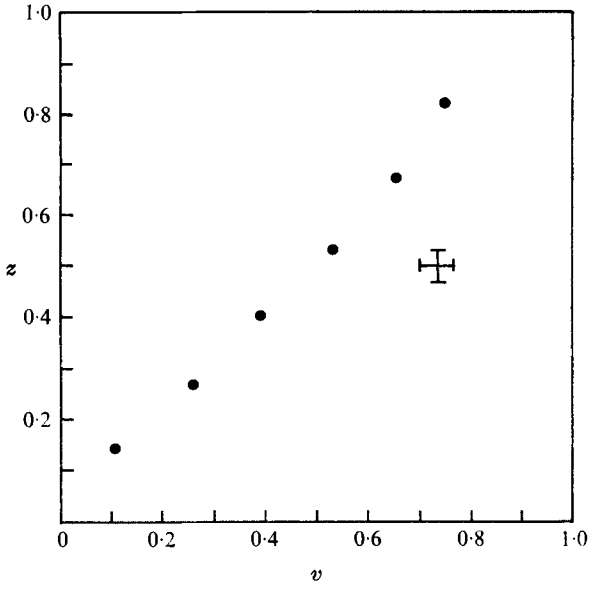

FIGURE 5. As for figure 4 with $S = 0{\cdot}63$, $\epsilon = 1{\cdot}3 \times 10^{-3}$ and $E = 4{\cdot}8 \times 10^{-4}$.

(figure 7) show no evidence of larger shears near the upper and lower boundaries than in the interior. We infer from these measurements that the top and bottom Ekman layers, present in the homogeneous case, are significantly weakened by the stratification, and that for large enough values of S the *interior* zonal velocity satisfies the top and bottom boundary conditions directly. Even for the case

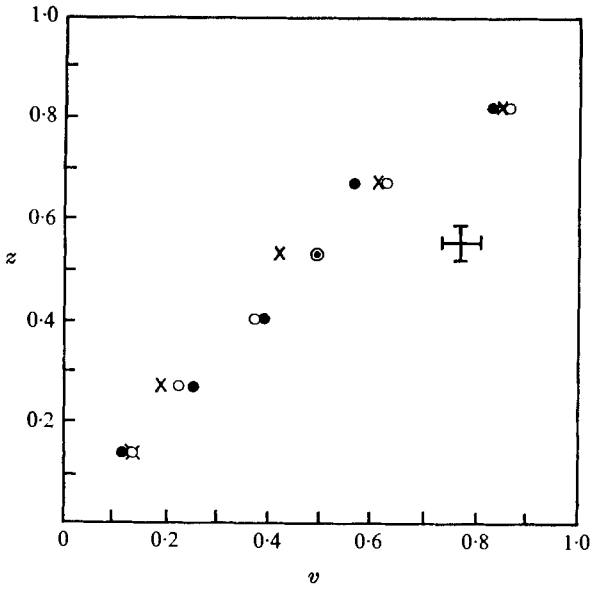

FIGURE 6. The same quantities as are shown on figure 3. Here $S = 0{\cdot}86$ and $E = 5{\cdot}2 \times 10^{-4}$. This plot shows profiles for three different Rossby numbers: ●, $\epsilon = 3{\cdot}7 \times 10^{-3}$; ×, $\epsilon = 5{\cdot}8 \times 10^{-3}$; ○, $\epsilon = 7{\cdot}5 \times 10^{-3}$.

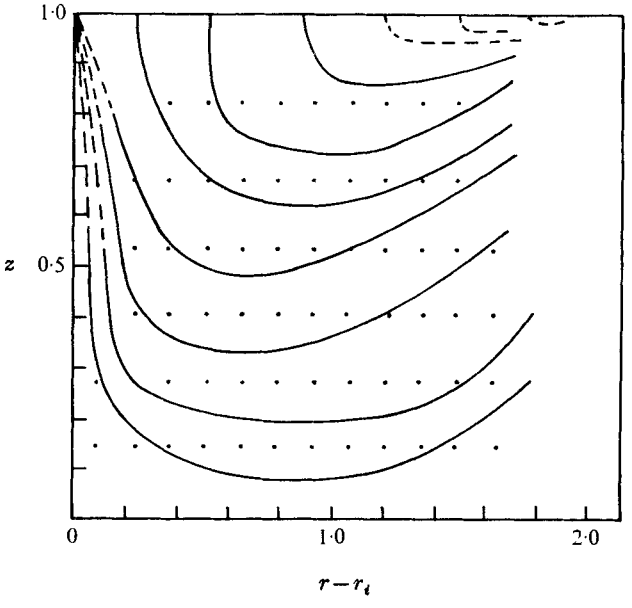

FIGURE 7. A contour plot of the zonal velocity v in the r, z plane for the case $S = 0{\cdot}86$, $\epsilon = 3{\cdot}7 \times 10^{-3}$ and $E = 5 \times 10^{-4}$. The velocity is normalized by setting $v(r_i, 1) = 0$, $v(r_0, 1) = 1$ and contours are drawn for $v = 0{\cdot}05$ and $v = 0{\cdot}1(0{\cdot}1)1{\cdot}0$. The points on the figure correspond to positions where measurements of v were obtained. The contours were positioned by eye through the data points, with a broken line used where there are insufficient data to do this with confidence.

$S = 0{\cdot}36$, the Ekman layer, if present, supports a much smaller shear than in the homogeneous case.

The interior zonal velocity also appears to satisfy the side-wall boundary conditions. In a homogeneous fluid there are side-wall boundary layers $O(E^{\frac{1}{3}})$ and $O(E^{\frac{1}{4}})$ in which the velocity has a large radial gradient. The field of view of the camera made it impossible to measure near both the inner and the outer wall of the annulus simultaneously, and so contour plots of v over the whole width of the annulus were not obtained. However, by comparing different runs it is concluded that the interior zonal velocity goes smoothly to its boundary values at both side walls.

It was not possible to get an accurate picture of the meridional circulation, for two reasons. First, the magnitudes of the velocities in the meridional plane are very small, and hence difficult to measure accurately. In fact, there was no visible evidence of vertical motion in any of the experiments. In the case of the radial velocity u a second difficulty arose from the presence, in some circumstances, of non-axisymmetric disturbances. These disturbances took the form of zonal waves and are discussed in more detail in § 5. They were present in the highest Rossby number flow shown in figure 6, and they provide the main contribution to the uncertainty in determining the zonal velocity in that case.

4. Time-dependent effects

The mean flow discussed in the previous section was measured when the system was judged to be in a 'steady' state. We now turn our attention to some time-dependent features of the flow. There are two aspects of interest: the initial spin-up of the fluid when the top is set in motion, and the long time effects due to diffusion of the density field. We shall deal with each aspect in turn.

In a stratified fluid, spin-up essentially occurs on two time scales. The shorter is the time scale $t_1 = O(E^{-\frac{1}{2}})$ corresponding to unstratified spin-up, which represents the initial adjustment to the motion of the top by the Ekman layers. This initial adjustment to a change in the velocity of the boundaries is a complicated process and has recently been the subject of a number of papers (e.g. Walin 1969; Buzyna & Veronis 1971; Saunders & Beardsley 1975; Barcilon *et al.* 1975). The final adjustment to the motion of the top takes place on the viscous time scale $t_2 = O(E^{-1})$. When S is large, the initial spin-up is restricted to a region near the boundary, and fluid at mid-depths feels the boundary motion on the viscous time scale t_2.

In order to examine this aspect of the flow the zonal velocity was measured at various times after the lid was set in motion. Figure 8 shows the results of one set of these measurements of v for the mid-radial position at a non-dimensional height $z = 0{\cdot}4$, plotted against the non-dimensional time. In this case $S = 0{\cdot}92$ and $\epsilon = 1{\cdot}6 \times 10^{-3}$. We see that a constant value of the velocity (within experimental error) is obtained for $t > 0{\cdot}4E^{-1}$. At $t = t_1$, the shorter time scale (marked by an arrow on figure 8), v is only about one-quarter of its final value. Consequently, in order to ensure that the flow is spun up it is necessary to wait

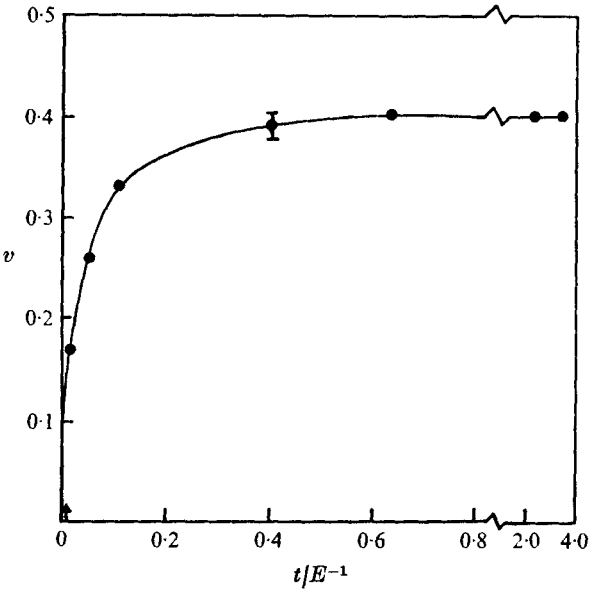

FIGURE 8. The non-dimensional zonal velocity v measured at $z = 0{\cdot}4$ plotted against the non-dimensional time t scaled by the Ekman number E.

some 6 h after the lid is set in motion for aqueous solutions in an annulus the size of the present apparatus.

Even when the fluid is spun up, it is not strictly in a steady state. Owing to the molecular diffusion of the density field, the presence of insulating top and bottom boundaries produces regions of reduced vertical density gradient near these boundaries. These regions increase in thickness with time, and eventually the whole fluid would become homogeneous. In these experiments the time scale $t = O(\sigma E^{-1})$ for this process is very much longer than the viscous time scale $t_2 = O(E^{-1})$ as $\sigma \sim 10^3$. The separation of these time scales allows the definition of a steady state to be taken as the flow existing at values of t for which $E^{-1} \ll t \ll \sigma E^{-1}$. Figure 8 also shows that the motion is steady on a time scale $O(E^{-1})$. One experiment was run until the effects of diffusion of the density field at the top and bottom boundaries would affect the stratification for $z \gtrsim 0{\cdot}75$ and $z \lesssim 0{\cdot}25$. It was found that there was a change in the zonal velocity in these outer regions, but no change could be detected in the interior.

It is appropriate at this point to note that, as is well known (see, for example, Greenspan 1968, p. 12), the diffusion of the density field produces a departure from solid-body rotation even when there is no driving by the lid. It was mentioned in § 2 that there was a large zonal flow present immediately after the filling of the tank was completed. A similar flow was also observed by Buzyna & Veronis (1971), when they filled a rotating cylinder with a stratified fluid. After waiting some 2–3 h this zonal motion had become very much reduced and it appeared that the transients introduced by the filling process had decayed. The remaining motion, assumed to be driven by the diffusion of the density field, was

measured in most of the experiments. At the relatively low rotation rates used ($\Omega < 1{\cdot}6$ rad/s) this flow was always small in comparison with that driven by the lid and it has been ignored in all the results presented in this paper.

5. Stability of the basic flow

The axisymmetric mean flow described above is susceptible to instability due to the growth of non-axisymmetric disturbances. Baroclinic instabilities can develop through the release of potential energy stored in the horizontal density gradient which is set up in response to the vertical shear (the thermal wind). The stability of the flow driven by a differentially rotating lid on an annulus has been examined by Pedlosky (1970) for the moderately stratified case $\sigma S < O(1)$. He found that there is a minimum shear above which the flow is unstable to non-axisymmetric disturbances. In the present experiment the shear is proportional to the Rossby number ϵ, and so we might expect the presence of non-axisymmetric disturbances at high enough Rossby numbers.

In order to determine whether non-axisymmetric disturbances were present in a given experiment the dye lines were examined at all available depths. It was not possible to assert unambiguously that a given flow possessed no such disturbances as there is always some small meridional circulation which deflects the dye from following a curve r = constant. However, provided the deflexion was unidirectional and did not significantly exceed that which could be produced by the meridional circulation the flow was designated as symmetric.

Seventeen experiments run at different values of ϵ and S were examined for the presence of non-axisymmetric disturbances. The results of these examinations are shown on figure 9, where the flows have been characterized by the presence or absence of waves. In the cases where this characterization could not be made unambiguously a third classification has been introduced. The ordinate $\epsilon/E^{\frac{1}{2}}$ on figure 9 represents the ratio of the viscous dissipation time to the circulation time, and so is a measure of rate of energy input to the perturbation compared with the dissipation rate. The abscissa is the stratification parameter S. We note that for a given S, the flow becomes non-axisymmetric at large values of $\epsilon/E^{\frac{1}{2}}$, and that the value of $\epsilon/E^{\frac{1}{2}}$ required for non-axisymmetric flow increases as S increases.

There appear to be no theoretical calculations of the stability of the basic flow for $\sigma S > O(1)$. However, it is useful to write down the potential-vorticity equation for the flow. This is of the form

$$\epsilon \frac{D}{Dt}\left(\zeta + \frac{2}{S}\right) = E\nabla^2\left(\zeta + \frac{2}{\sigma S}\right), \tag{5.1}$$

where ζ is the vertical component of the vorticity and D/Dt the material derivative. In axisymmetric steady flow the left-hand side of the equation is small when $\sigma S > \epsilon$ (Pedlosky 1970) and the effect of the stratification is determined by the parameter σS. On the other hand if the flow is unsteady or non-axisymmetric, provided $E < \epsilon$, which is the case in the present experiments, the right-hand side

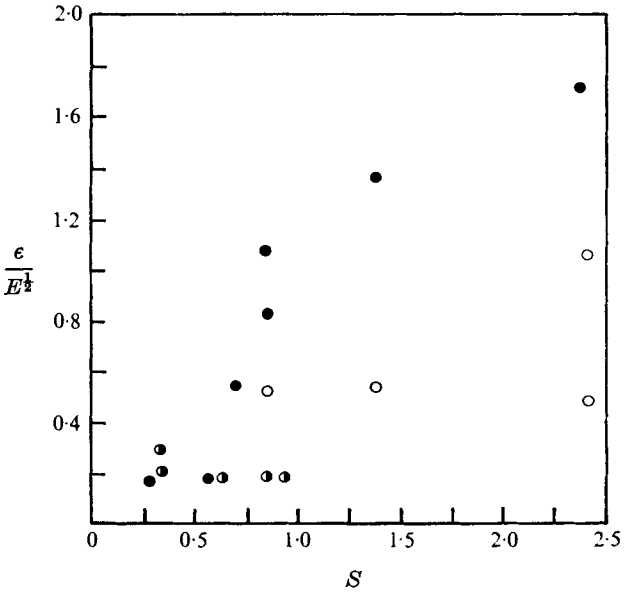

FIGURE 9. Classification of the flow. ○, axisymmetric flow; ●, non-axisymmetric disturbances present; ◑, classification uncertain. One experiment ($S = 17{\cdot}9$, $\epsilon/E^{\frac{1}{2}} = 4{\cdot}0$) is not shown on the figure: the flow was axisymmetric in that case.

of the equation is negligible and (5.1) reduces to

$$\frac{D}{Dt}\left(\zeta + \frac{2}{S}\right) = 0,$$

expressing conservation of potential vorticity. Then the effect of the stratification is determined by S. Thus it would seem to be possible that, even though $\sigma S \gg 1$, baroclinic instability could occur when S is not too large.

An example of these non-axisymmetric motions is shown on figure 10 (plate 1). This example, which is fairly typical, has a zonal wavenumber of about 10, although as can be seen the structure of the wave motion varies with radius. The motions appeared to be along isopycnal surfaces, and there was no evidence of any vertical mixing.

6. Conclusions

The flow of a stratified fluid in a rotating annulus with insulating boundaries driven by a differentially rotating lid has been investigated experimentally. When the stratification is large enough the interior zonal velocity has an $O(1)$ vertical shear, and the Ekman layers appear to play no significant role in the dynamics. Also the side-wall boundary layers present in a homogeneous fluid appear to be absent when the fluid is strongly stratified. When the Rossby number of the motion is small enough the flow is axisymmetric.

The transient response of the flow to the motion of the lid confirms this picture. With the vertical Ekman pumping inhibited by the stratification the dominant mechanism for coupling the boundary driving to the interior flow, namely the

stretching of interior vortex lines, is lost. Consequently, the spin-up occurs on the time scale $t = O(E^{-1})$ associated with the viscous stresses. When the Rossby number of the flow is increased the flow becomes non-axisymmetric. These non-axisymmetric disturbances take the form of baroclinic waves, with a zonal wavenumber of about 10, which propagate around the annulus.

As has been mentioned in § 3, the large Prandtl number of the stratification has made it impossible to study the transition from the homogeneous to the stratified case, when $\sigma S \sim E^{\frac{1}{2}}$. The current experiments apply only to the strongly stratified case $\sigma S \gtrsim O(1)$. In this limit the results of the experiments are in basic agreement with the calculations of Barcilon & Pedlosky (1967) and Allen (1972, 1973). In his second paper, Allen investigated numerically some effects of non-linearities on the axisymmetric flow. For the smallest value of the Rossby number (0·01) he used in his calculations $\epsilon/E^{\frac{1}{2}} = 0{\cdot}4$, and so the results shown in § 5 would suggest that the flow would be non-axisymmetric unless $S > 1$. As most of his calculations were carried out for $\epsilon = 0{\cdot}1$ and $S = 1{\cdot}1$ the effects of nonlinearity introduced at these values of the Rossby number may be secondary to the effect of baroclinic waves travelling around the annulus.

The experiments were carried out whilst I was visiting the Department of Aerospace Engineering, University of Southern California. I am grateful to Professor T. Maxworthy for inviting me to work in his laboratory and allowing me free use of the experimental facilities. The work was supported by the British Admiralty and the National Science Foundation through the International Decade of Ocean Exploration, grant no. NSF-IDO-74-15063.

REFERENCES

ALLEN, J. S. 1972 Upwelling of a stratified fluid in a rotating annulus: steady state. Part 1. Linear theory. *J. Fluid Mech.* **56**, 429–445.

ALLEN, J. S. 1973 Upwelling of a stratified fluid in a rotating annulus: steady state. Part 2. Numerical solutions. *J. Fluid Mech.* **59**, 337–368.

BAKER, D. J. 1966 A technique for the precise measurement of small fluid velocities. *J. Fluid Mech.* **26**, 573–575.

BARCILON, A., LAU, J., PIACSEK, S. & WARN-VARNAS, A. 1975 Numerical experiments on stratified spin-up. *Geophys. Fluid Dyn.* **7**, 29–42.

BARCILON, V. & PEDLOSKY, J. 1967 Linear theory of rotating stratified fluid motions. *J. Fluid Mech.* **29**, 1–16.

BUZYNA, G. & VERONIS, G. 1971 Spin-up of a stratified fluid: theory and experiment. *J. Fluid Mech.* **50**, 579–608.

GREENSPAN, H. P. 1968 *The Theory of Rotating Fluids.* Cambridge University Press.

OSTER, G. 1965 Density gradients. *Sci. Am.* **213**, 70–76.

PEDLOSKY, J. 1970 Flow in rotating stratified systems. *Notes on* 1970 *Summer Prog. Geophys. Fluid Dyn., Woods Hole Ocean. Inst.*, no. 70–50, vol. 1, pp. 1–67.

SAUNDERS, K. D. & BEARDSLEY, R. C. 1975 An experimental study of the spin up of a thermally stratified rotating fluid. *Geophys. Fluid Dyn.* **7**, 1–28.

TAYLOR, G. I. 1917 Motion of solids in fluids when the flow is irrotational. *Proc. Roy. Soc.* A **93**, 99–113.

WALIN, G. 1969 Some aspects of time-dependent motion of a stratified rotating fluid. *J. Fluid Mech.* **36**, 289–307.

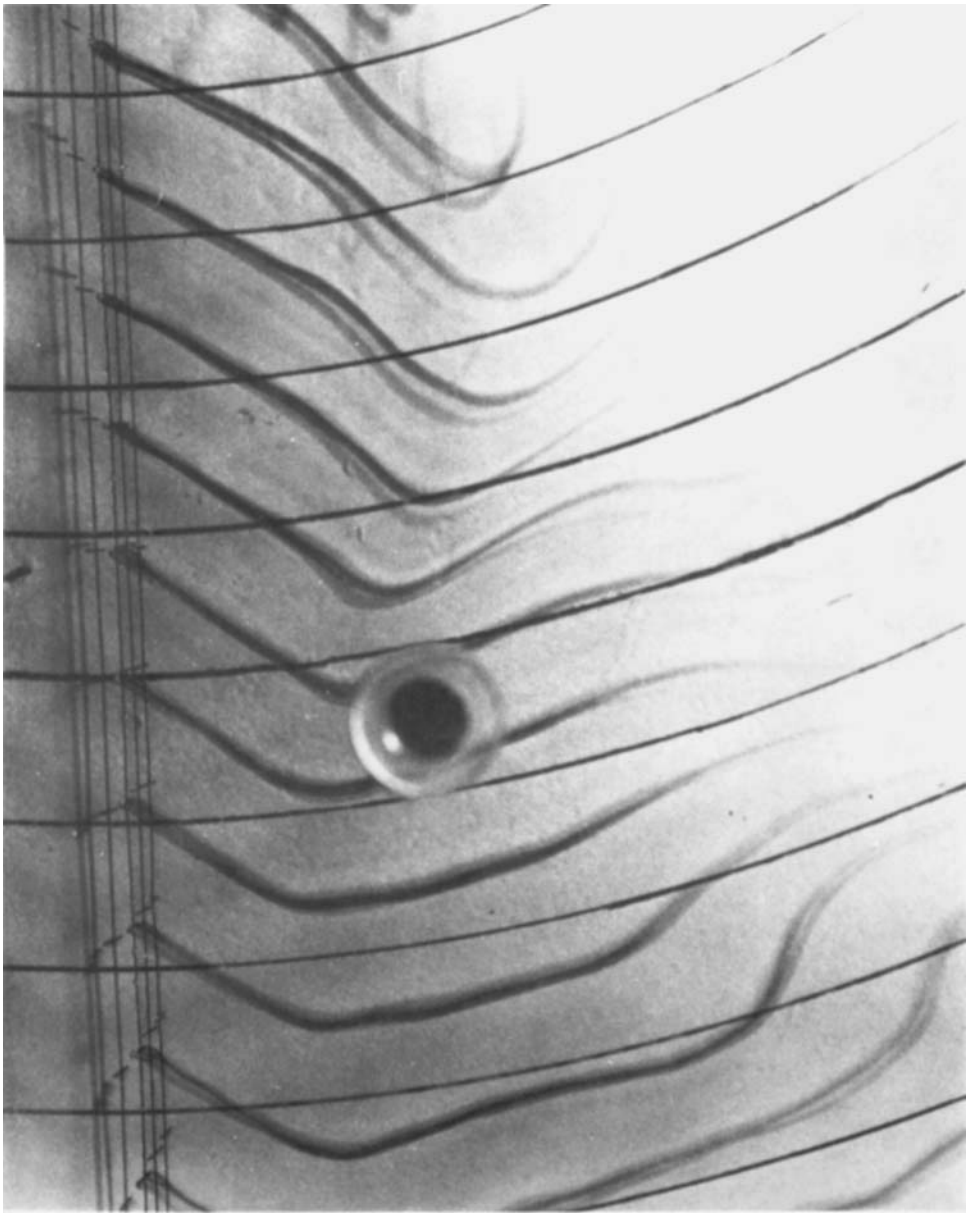

FIGURE 10. Non-axisymmetric motions at $z = 0{\cdot}4$ revealed by dye streaks. For this run $\epsilon = 1{\cdot}6 \times 10^{-3}$, $S = 0{\cdot}27$ and the zonal wavenumber is about 10. The lines on the bottom at the tank are 2·54 cm apart, and the circular mark is a hole drilled into the top of the lid.